AD NUMBER: AD0085427	
CLASSIFICATION CHANGES	
TO:	Unclassified
FROM:	Confidential
LIMITATION CHANGES	
TO:	Approved for public release; distribution is unlimited.
FROM:	Distribution authorized to U.S. Gov't. agencies and their contractors; Administrative/Operational Use; 20 Apr 1954. Other requests shall be referred to the Air Force Research and Development Command, Project RAND, Washington, DC 20330
AUTHORITY	
	30 Apr 1966 DoDD 5200.10, gp-4; 6 Sep 1966, USAF via Rand Ltr

CONFIDENTIAL

CONFIDENTIAL

U.S. AIR FORCE

Project RAND

FC

RESEARCH MEMORANDUM

SEE TITLE PAGE FOR DISTRIBUTION RESTRICTIONS

The RAND Corporation
SANTA MONICA · CALIFORNIA

CONFIDENTIAL

CONFIDENTIAL

U. S AIR FORCE

PROJECT RAND

RESEARCH MEMORANDUM

(Uncl) DETECTION RANGE OF AN ACTIVE RADAR SEEKER

J. D. Mallett
P. Swerling

RM-1238

20 April 1954

Copy No. 26

Assigned to ______________________

DISTRIBUTION RESTRICTIONS

No restrictions on further distribution, other than those imposed by security regulations.

The RAND Corporation
1700 MAIN ST. • SANTA MONICA • CALIFORNIA

CONFIDENTIAL

Addendum to RM-1238: Detection Range of an Active Radar Seeker

by J. D. Mallett and P. Swerling

In the List of Symbols, p.v, insert:

Symbol	Definition	Page First Used
V_c	closing velocity of the target with respect to the seeker	7

SUMMARY

This report analyzes the effect of various factors on the detection range of an active radar seeker. The factors considered include those which define the performance of a seeker, such as size of the search pattern, range and angular resolution, range of possible target velocities (with respect to the seeker), target closing velocity, target echoing area, false alarm time, and probability of detection; and constants describing the seeker such as average transmitted power, wavelength, dish size, pulse repetition rate, pulse width, scan time, i-f and a-f bandwidth, and number or range gates and velocity channels.

Equations and curves are developed to show the variation of detection range with the above-mentioned parameters, and to aid in making optimum choice of scan time.

TABLE OF CONTENTS

LIST OF SYMBOLS

Symbol	Definition	Page First Used
D	dish diameter	2
G_R	receiver gain	2
G_T	transmitter gain	2
g	scale factor	5
I	fraction of transmitter power that leaks over into receiver	16
k	**Boltzmann's constant**	2
K	$K = \frac{\Delta V R_o}{m V_c}$	10
L	system losses	2
m	number of beam positions in search pattern	4
n	false alarm number	3
N	effective number of samples integrated by the **audio** filter	3
$\overline{NF}$	receiver noise figure	2
$\bar{P}$	average transmitter power	2
p	effective number of range gates	4
P_b	blip-scan ratio	3
P_{bav}	average single-scan probability of detection	9
P_c	cumulative probability of detection	8
P_{cav}	average cumulative probability of detection	8
q	number of velocity channels used to cover the velocity uncertainty	4

LIST OF SYMBOLS Cont'd

Symbol	Definition	Page First Used
R	range	2
R_o	range at which $\bar{x} = 1$	3
R_a	range for $P_{cav} = 90\%$ at optimum scan rate	12
R_b	range for $P_{bav} = 90\%$ at optimum scan rate	14
t	time on target for a single scan	4
T	time to complete a single scan of the search volume	4
ΔV	equivalent c-w i-f bandwidth (defined more precisely on p. 2)	2
$\bar{x}$	average i-f signal to noise power ratio for a fluctuating target	2
Y_b	voltage threshold	
β	fraction of transmitter power which is noise per cycle of bandwidth	16
δ	radial distance moved by target in time T	7
ξ	$\xi = \frac{K}{R_o} = \frac{\Delta V}{V_c^m}$	12
λ	wavelength	2
θ	beamwidth	4
θ_H	azimuthal sector searched	4
θ_V	elevation sector searched	4
σ	instantaneous target echoing area	5
$\bar{\sigma}$	average of σ for a fluctuating target	2
τ_{fa}	false alarm time	4

I. PARAMETERS RELEVANT TO SEEKER PERFORMANCE

The purpose of this report is to set down the factors that must be considered in determining the theoretical range of a seeker, to present graphs which show how these factors affect detection range and which aid in choosing optimum parameters, and to apply these results to a few particular cases felt to be representative of actual or proposed seekers.

In general a seeker's performance can be defined by tactical considerations such as the following:

1. The space volume searched.
2. The velocity and acceleration uncertainty - i.e. the range of possible target velocities and accelerations (relative to the seeker) over which the seeker can operate.
3. The closing velocity.
4. The false alarm time.
5. The probability of detection at various ranges, under various conditions of search.
6. Resolution and accuracy.
7. Target echoing area.

To achieve the required performance, the values of various quantities such as transmitted power, wavelength, dish size, repetition rate and pulse width (in a pulsed system), scan time, missile speed, and number of velocity and range channels can be chosen within certain physical limitations.

The physical limitations imposed on the seeker are usually size (principally of the dish), power, and complexity. It is desirable to know how the seeker performance, especially with respect to search, is affected by these physical limitations.

One might start a discussion of this subject with the radar range equation:

(1) $$R^4 = \frac{\bar{P}\, G_R G_T\, \lambda^2\, \bar{\sigma}}{(4\pi)^3\, \bar{x}\, \Delta V\, k\, T\, \overline{NF}\, L}$$

One can rewrite this to include the more interesting parameter, dish diameter D:

(1') $$R^4 = \frac{(7.4)^2\, \bar{P}\, D^4\, \bar{\sigma}}{(4\pi)^3\, \bar{x}\, \Delta V\, \lambda^2\, kT\, \overline{NF}\, L}$$

This equation applies to either a pulsed or a c-w system. (Definitions of symbols are on pp. iv and v.)

For c-w systems, ΔV is the i-f bandwidth. For pulsed systems (assuming i-f bandwidth $\approx$ reciprocal of pulse width) ΔV is the pulse repetition frequency; or, if there is comb filter integration in the i-f, it is the width of the filter around each harmonic component of the signal.

The range equation as stated in (1) or (1') does not explicitly involve many of the parameters which determine performance. Closing velocity, velocity uncertainty, search angle, scan time, false alarm time, and probability of detection enter implicitly into the range equation because they affect the value of $\bar{x}$. If one knows the values of these parameters, $\bar{x}$ can be computed.

Due to the complicated nature of the dependence of $\bar{x}$ on these quantities, it seems that the best way to approach the problem of relating these parameters to seeker performance is to give a series of curves plotting the relation of some of the parameters to others.

II. BLIP - SCAN CURVES

A basic piece of information in any such discussion is the blip-scan curve, which shows the relation between the blip scan ratio, P_b, and $\frac{R}{R_o}$. (Blip scan ratio is the ratio of number of blips to number of scans when a target is present at a fixed range. The ratio states the probability of a blip appearing on a single scan when a target is present at a given range.)

R_o is defined by setting $\bar{x}$ equal to unity in (1') :

$$R_o^4 = \frac{(7.4)^2 \bar{P} D^4 \bar{\sigma}}{(4\pi)^3 \Delta V \lambda^2 kT \overline{NF} L} \tag{2}$$

It is possible from Refs. 1 and 2 to obtain curves of P_b vs $\frac{R}{R_o} = \left(\frac{1}{\bar{x}}\right)^{1/4}$ for various values of the parameters N and n.

N is the effective number of samples, in which the noise samples can be considered statistically independent of each other, integrated by the audio filter. Strictly speaking, Refs. 1 and 2 compute blip-scan curves only for pulsed systems, and then only for the case where integration consists simply of adding N pulses. It is assumed here that the resulting blip-scan curves can be applied approximately to the case of a scanning beam, for either pulsed or c-w systems, provided an equivalent value of N is judiciously chosen.* If it be assumed that the audio filter integration

*The difference between pulsed and c-w systems can be shown to be small since a pulsed system using range gates behaves after gating almost like a c-w system as far as signal-to-noise ratio is concerned. The main approximation is concerned with the assumption that N equal pulses added together are equivalent to a number of pulses integrated by means of a filter.

time is roughly equal to t, the time during which the target is within the half power points of the beam during a single scan, then the value of N can be taken to be roughly

$$N \approx t\,\Delta V \tag{3}$$

The number of effectively independent noise samples occurring in the false alarm time τ_{fa}, before audio filtering, is denoted by n. Hence,

$$n \approx \tau_{fa}\,\Delta V\,q\,p \tag{4}$$

Here q is the number of velocity channels used to cover the velocity uncertainty, and p is the number of range gates used. For c-w systems p is equal to unity. This actually makes little difference in detection range as compared with pulsed systems where p is fairly large, **because range** for a given blip-scan ratio is a relatively insensitive function of n.

One can rewrite the formula for N

$$N = t\,\Delta V = \frac{T\,\Delta V}{m} \tag{5}$$

$$m \approx \frac{\theta_V \theta_H}{\theta^2} \approx \theta_V \theta_H \left(\frac{D}{1.27\lambda}\right)^2 \tag{6}$$

Here T is the scan time (i.e. time in which the beam completes one search pattern) and m is the number of beamwidths included in the search pattern. Eqs. 2 to 6 now relate many of the tactical parameters to N, n, and R_o.

Figures 1 and 2 can be used to calculate curves of blip-scan ratio vs

R/R_o for various values of N and n, for a particular fluctuating target model. (The target echoing area is considered to fluctuate according to the distribution: $w(\sigma, \bar{\sigma}) = \frac{1}{\bar{\sigma}} e^{-\sigma/\bar{\sigma}}$. The echoing area is considered to be constant for the time on target during a single scan, $\frac{T}{m}$, but to fluctuate independently between scans.) It has been found numerically* and shown mathematically[2] that, for this target fluctuation model, the blip-scan curves for various values of N and n can be represented to a good approximation by a single curve of blip-scan ratio vs u, where $u = \frac{R}{R_o} \cdot g(n,N)$. Here g(n,N) is a scale factor depending on n and N. The deviation of this from the actual curves is small enough to be ignored over a parameter range of $n = 10^4$ or higher, N = 1 to about 1000, and blip-scan ratio greater than about one percent; this is the usual range of interest. Figures 1 and 2 give, respectively, the curve of blip-scan ratio vs u and the scale factor g(n,N).

III. DETECTION CRITERIA

One can now proceed to define whatever detection criterion is thought to be desirable--for example, one can consider a target detected if a blip appears on a single scan, or on two successive scans, etc.

The criterion considered to be of most interest here is the single blip criterion. For an automatic device like a seeker employing rejection of ground clutter by filtering, it appears that a good way to operate is to use a fairly high threshold, insuring a low probability of false alarm due to noise, and then to take action on the first crossing of the threshold. Such

---

*By R. H. Dishington in an internal RAND working paper.

action might be to stop the seeker and examine more carefully the point in space at which the blip appears. The high threshold will assure infrequent false stoppings of the seeker.

With the false alarm probability extremely low, one may say that stopping the antenna is essentially the same as committing the missile. One could instead use a lower threshold and allow the antenna to be stopped fairly often due to noise. When the blips were found to be noise by further tests the antenna could again be put into search. This would be an inefficient way to operate because of the time lost in starting and stopping the antenna. One could also use a two or more successive blip criterion for detection. It has been found, however, that the sensitivity with the two-blip criterion is not quite as good as with the one blip criterion, when adjusted to give the same overall probability of detection and of false alarm. To date, as far as we know, no criterion involving multiple successive blips has been found that surpasses the one-blip criterion in sensitivity for the same overall probability of detection and false alarm time.*

One may be interested in the following cases:

a. The seeker is turned on for many search periods so that there is the possibility of many different looks at the target.

b. The seeker is turned on for only one **search period.**

If sensitivity is the prime consideration one would use many scans, especially when the target is fluctuating. There are, however, certain

---

*Other methods of detection are sometimes useful for reasons other than sensitivity of detection of signal in noise. For instance, a double threshold method of detection is useful because it discriminates against "railing" or single-pulse types of interference while lowering sensitivity of detection only slightly.

considerations that make it desirable not to turn on the seeker at too long a range. One is that the wrong target might be acquired. Another is that the target may have a sensing device that tells it when the seeker is turned on and enables it to take evasive action. Evasive action is especially important when the seeker is directed at a low-flying target and when the difference between target and ground radial velocities is being used to distinguish between signal and ground clutter. If sufficient time is allowed for maneuvering, the target may turn so as to make its signal have the same frequency as the ground clutter, thus making detection very difficult.

The most interesting case here appears to be to allow the seeker to accumulate looks over a distance such that any increase in distance would make only a slight improvement and, at the same time, little maneuvering is possible in the time required to close. For case a, it is assumed that the seeker is turned on when the target is at a range of approximately 2 R_o. This gives an accumulation distance which is probably in the region of interest.

IV. AVERAGE CUMULATIVE PROBABILITY OF DETECTION AND AVERAGE SINGLE SCAN PROBABILITY OF DETECTION

A target moving with constant radial velocity V_c toward the seeker will move a certain distance $\delta(R)$ during each search period. The target is said to be detected by the time it reaches a certain range R from the seeker, if a blip has occurred on at least one scan up to the time the target has reached range R.

The basic piece of information in which one is interested is the probability of detection by a given range R (i.e. by the time the target has reached a given range R).

Consider case a, where the seeker is turned on for many search periods. Let $P_b(R)$ be the blip-scan ratio at range R. Then, if the last look at the target happens to occur precisely at range R, the probability of detection by range R will be

(9) $$P_c(R) = 1 - \prod_{i=1}^{k} \left[1 - P_b(R + i\delta(R))\right]$$

P_c is called the cumulative probability of detection by range R. Here k is chosen such that $R + k\delta$ is between $2R_o$ and $2R_o + \delta$. This was chosen because, usually, beyond this point the probability of a blip appearing due to noise is just about as large as the probability of a blip appearing due to a target.

P_c is still not the thing one wants to know. For a given range R, it will rarely happen that the target motion is such that the last look* will occur precisely when the target is at range R. In fact, the last look has equal probability of occurring anywhere in the range R to $R + \delta(R)$. Therefor the quantity of interest is $P_{cav}(R)$, the average cumulative probability of detection at range R:

(10) $$P_{cav}(R) = \frac{\int_R^{R+\delta(R)} P_c(r)\,dr}{\delta(R)}$$

Similarly, in case b, if the seeker is turned on for just one search period, the interesting quantity would be $P_{bav}(R)$, the average single-scan

---

*That is, the last look before the target gets closer than range R.

probability of detection at range R:

$$(11) \qquad P_{bav}(R) = \frac{\int_{R}^{R+\delta(R)} P_b(r)\, dr}{\delta(R)}$$

Examples of these curves for different parameter values are shown in Figs. 10, 11, 12, and 13, so that one can see the difference between the cumulative and single-scan cases, for instance, and the effect of averaging the blip-scan curve for a given closing velocity.

These curves were plotted using parameter values that have been suggested for actual seeker applications. One would like, however, to find any optimum parameter values that exist, within given restraints, and to see how performance varies with all the parameters. The choise of scan time, for instance, involves an optimization since too long a scan time reduces detection range because of averaging, as in (10) and (11), while too short a scan time reduces integration. To this end, a set of curves was developed to obtain optimum scan time and to show the performance variation with the various parameters. These curves are shown in Figs. 3 through 9. They are made for an average cumulative probability of detection $P_{cav} = 90\%$ and for an average single-scan probability of detection $P_{bav} = 90\%$. The 90% probability level is believed to be in the region of interest for a missile seeker. The value of n is taken to be 10^7, which corresponds to a τ_{fa} of around 700 seconds. The results can readily be obtained for a different value of n, if desired.

V. OPTIMUM SCAN RATE; VARIATION OF RANGE WITH OTHER PARAMETERS

As has been stated, the blip-scan ratio vs $\frac{R}{R_0}$ curves can be represented as a curve of blip-scan ratio vs u, where $u = g \cdot \frac{R}{R_o}$, g depending on n and N. Cumulative probability of detection for various values of the interval $\delta(R)$ can also be represented as curves of cumulative probability of detection vs u for various values of $\delta(u)$. Here

(12) $$\delta(u) = g \cdot \delta(\frac{R}{R_o}) = \frac{g}{R_o}\,\delta(R) = \frac{g V_c T}{R_o}$$

Two such cumulative probability curves, as well as the blip-scan curve, are shown in Fig. 1.

These curves can also be averaged over an interval $\delta(u)$ to give curves of average cumulative probability of detection P_{cav} vs u, or average single-scan probability of detection P_{bav} vs u, for various values of $\delta(u)$. Figure 3 is a curve of u vs $\delta(u)$ for a fixed average cumulative probability of detection $P_{cav} = 90\%$. Figure 7 is a curve of u vs $\delta(u)$ for average single-scan probability of detection $P_{bav} = 90\%$.

The effect of scan time T on range performance can be shown as follows: T influences both N and δ :

(13) $$\begin{cases} \delta(\frac{R}{R_o}) = \frac{V_c T}{R_o} \\ N = \frac{T\Delta V}{m} \end{cases}$$

Combining these,

(14) $$N = K\,\delta(\frac{R}{R_o})$$

$$\text{where } K = \frac{R_o \Delta V}{m V_c}$$

Now, if one fixes K and n, a curve of $\frac{R}{R_o}$ vs $\delta(\frac{R}{R_o})$ for $P_{cav} = 90\%$ or for $P_{bav} = 90\%$ can be obtained as follows: each choice of $\delta(\frac{R}{R_o})$ determines N by (14); g can then be obtained from Fig. 2; then $\delta(u) = g \cdot \delta(\frac{R}{R_o})$ can be obtained; Fig. 3 or Fig. 7 is then used to get u; and finally u is converted to $\frac{R}{R_o}$ by $u \quad g \cdot \frac{R}{R_o}$. The result is a curve of $\frac{R}{R_o}$ vs $\delta(\frac{R}{R_o})$ for fixed K and n, and $P_{cav} = 90\%$ or $P_{bav} = 90\%$. Since scan time is not involved in R_o, one can regard these curves as showing the effect of scan time on range for $P_{cav} = 90\%$ or $P_{bav} = 90\%$. Figure 4 shows a set of such curves for $n = 10^7$, $P_{cav} = 90\%$, and various values of $K = \frac{R_c \Delta V}{V_c m}$. Figure 8 shows similar results for $P_{bav} = 90\%$.

Two important conclusions can be drawn from Figs. 4 and 8. First, the optimum value of $\delta(\frac{R}{R_o})$ is approximately equal to .06 for $P_{cav} = 90\%$, and to .20 for $P_{bav} = 90\%$. This is practically independent of K for $100 \leq K \leq 2000$. Second, the effect of scan time on range is slight when scan time is varied from optimum by as much as a factor of two either way.

Figures 5 and 9 give an alternative way of plotting the same information. Given R_o, ΔV, V_c, and m, one can find from these curves the range for $P_{cav} = 90\%$ or $P_{bav} = 90\%$. For $P_{cav} = 90\%$, this is plotted for $\delta(\frac{R}{R_o}) = .06$ (the optimum) as well as for $\delta(\frac{R}{R_o}) = .15$ to show the penalty for non-optimum $\delta(\frac{R}{R_o})$. For $P_{bav} = 90\%$, the curves are given for $\delta(\frac{R}{R_o}) = .20$ (optimum) and for $\delta(\frac{R}{R_o}) = .40$.

Figure 6 is still another set of curves which can be derived from Fig. 4 or Fig. 5. It is plotted for $\delta(\frac{R}{R_o}) = .06$. From Fig. 6, after choosing the desired range for $P_{cav} = 90\%$, as well as choosing speed, search pattern, and i-f bandwidth, one can find R_o, from which the necessary transmitted power can be determined.

Figure 6 is actually two plots in one. R (for P_{cav} = 90%) is plotted against R_o for $\xi = \frac{K}{R_o} = \frac{\Delta V}{mV_c}$ held constant; also R is plotted against ξ for R_o constant. This allows easy interpolation.

No curve corresponding to Fig. 6 is given for P_{bav} = 90%.

Having determined the optimum value of $\delta(\frac{R}{R_o})$, one would like to know how range varies with the other parameters. Since the results for P_{cav} = 90% differ from those for P_{bav} = 90%, it is best to discuss these two cases separately. The results for P_{cav} = 90% will be discussed in greater detail; corresponding results for P_{bav} = 90% will be summarized later on.

A. P_{cav} = 90%

In equations (15) through (19), R_a represents the range for P_{cav} = 90% when the scan time is optimum--i.e., $\delta(\frac{R}{R_o})$ = .06.

If Fig. 5 were plotted on log-log paper, it would turn out that for $K \leqq 400$, and $\delta(\frac{R}{R_o})$ = .06, the K vs $\frac{R}{R_o}$ curve is approximately a straight line with a slope of 4.

Thus one can write

(15) $$R_a \propto R_o K^{1/4}$$

Since $K = \xi R_o$, this could be expressed

(16) $$R_a \propto \xi^{1/4} R_o^{5/4}$$

If one writes $R_a \propto \xi^{\gamma} R_o^{\phi}$, then it can be seen from Fig. 6 that γ = 1/4, ϕ = 1.25 gives a good approximation for $R_o \leqq 15$, $\xi \leqq 30$. For K > 400, better values of γ and ϕ could be chosen from Fig. 6.

CONFIDENTIAL

Substituting for ξ and R_o in (16),

$$(17) \qquad R_a^{\,4} \propto \frac{\bar{P}^{\,5/4}\, D^3\, \bar{\sigma}^{\,5/4}}{V_c\, \theta_V \theta_H\, \lambda^{1/2}\, (\Delta V)^{1/4}\, (kT\, \overline{NF}\, L)^{5/4}}$$

for $K \leq 400$.

The variation of R_a with ΔV is significant for the following reason: A certain frequency band is required to cover the velocity uncertainty (range of possible target velocities) in a doppler system. ΔV can, however, be reduced by introducing multiple velocity channels. This improves range performance, but the multiple channels are costly to build; hence one is interested in how much the range performance is actually improved. Since ΔV varies as the inverse of q, the number of velocity channels, one can see from (17) that, in the region of approximation considered,

$$(18) \qquad R_a \propto q^{1/16}$$

From Fig. 5 it can be seen, however, that as K increases, the exponent of q in (18) will get larger than 1/16. In fact, for large K ($K > 1000$), the variation would be closer to

$$(19) \qquad R_a \propto q^{1/8}$$

There is, therefore, more payoff in increasing q when K becomes larger. From Fig. 6 one could in fact compute the actual gain in introducing more velocity channels for given values of ξ and R_o.

Another interesting point is the strong dependence of R_a on dish diameter, and the fairly strong dependence on closing velocity and search angles.

CONFIDENTIAL

These parameters are more significant than λ or q.

B. $P_{bav} = 90\%$

In equations (20) through (23), R_b represents the range for $P_{bav} = 90\%$, when scan time is optimum--i.e., $\delta(\frac{R}{R_o}) = .20$.

If Fig. 9 were plotted on log-log paper, it would turn out that for $K \geq 100$, and $\delta(\frac{R}{R_o}) = .20$, the K vs $\frac{R}{R_o}$ curve is approximately a straight line with a slope of 5.5.

Thus one can write

(20) $$R_b \propto R_o \, K^{1/5.5}$$

Since $K = \xi R_o$, this could be expressed

(21) $$R_b \propto \xi^{1/5.5} \, R_o^{1.18}.$$

Substituting for ξ and R_o in (21),

(22) $$R_b^4 \propto \frac{\bar{P}^{1.18} \, D^{3.27} \, \bar{\sigma}^{1.18}}{(\theta_V \theta_H)^{.73} \, v_c^{.73} \, (\Delta V)^{.45} \, (kT \, \overline{NF} \, L)^{1.18}}$$

for $K \geq 100$.

Hence, for this range of parameters,

(23) $$R_b \propto q^{.11}$$

For $K < 100$, the variation of R_b with q becomes less sensitive than in (23).

C. Miscellaneous Observations

An assumption implicit in the treatment thus far is that the target spectrum is narrow compared to the pass band of the post-detection integrating filter. This is necessary in order to be consistent with the assumed target fluctuation model--i.e., independent fluctuation from scan to scan but no fluctuation during the time on target for one scan. Since target spectra appear to have the major part of their energy in a frequency range corresponding to 2-10 mph, this does not seem to be an unreasonable assumption. However, one might be interested in the cases where the filter width is narrow compared to the target spectrum, or where the filter and the target spectrum are of approximately equal width. Therefore a blip-scan curve, an average cumulative probability of detection curve, and an average single-scan probability of detection curve were computed using a rapidly fluctuating target model in which the fluctuations are independent from pulse to pulse (or in the c-w case, the fluctuation spectrum is comparable in width to ΔV); this represents an extreme case. The results are shown in Fig. 14. While this curve crosses that of Fig. 10 (the comparable case for a slowly fluctuating model), Fig. 14 shows an improvement at $P_{cav} = 90\%$. Hence it can be deduced that in a case intermediate between these two extremes, the range, at $P_{cav} = 90\%$, will probably be greater than predicted by the curves of Figs. 1 - 13.

In computing the range of a seeker, assumptions must be made about the noise figure, losses, and maintenance degradation. Estimates of these are the following:

Beam shape loss due to the fact that time on target was computed on the basis of half-power one-way beamwidth . . . . . 3 db

Loss due to cross polarization or circular polarization or "magic tee" (applies only for an active c-w system). . . . . 6 db

Two-way radome loss . . . . 2 db

Two-way plumbing loss . . . . 2 db

Maintenance degradation . . . . 4 db

The noise figure varies considerably; 10-13 db is usual for a microwave system using an i-f. A c-w system without i-f can be much worse, but can do as well as 18 db. Hence $\overline{NF} \cdot L$ might for a c-w system be between about 27 db and 35 db.

Figures 10, 11, 12, and 13 give curves of P_b, P_{bav}, and P_{cav} for possible c-w systems. The effect on P_b, P_{bav}, and P_{cav} when some of the parameters are varied can be seen by comparing these curves. The cross at the 90% point indicates the range for optimum scan time for $P_{cav} = 90\%$; the circle indicates the range for optimum scan time for $P_{bav} = 90\%$. Thus one can see how far from optimum the actual curves are.

One of the most serious limitations on active c-w seeker range is the limit imposed by transmitter noise and leakage to the receiver.

If β = fraction of transmitter power that is noise in each cycle of bandwidth, and I = fraction of transmitter power that leaks over to the receiver, then $\bar{P}\beta I$ is the average noise power per cycle in the receiver due to this leakage. The quantity $kT\overline{NF}$ is the average noise power per cycle due to circuit noise in the receiver. It is clear that once the leakage noise, which is proportional to $\bar{P}$, surpasses the circuit noise, it does not help much to increase $\bar{P}$, since noise is increased proportionately.

This also affects the validity of the equations describing the variation of range with $\overline{P}$ (Eqs. 1, 1', 2, 17, and 22). In order for these equations to be strictly correct, one should replace the quantity $kT\overline{NF}$ by the quantity $kT\overline{NF} + \beta I\overline{P}$. Thus, as long as $\beta I\overline{P}$ is small compared with $kT\overline{NF}$, the equations remain valid as they stand. As $\overline{P}$ increases, however, a point is eventually reached where no additional improvement in range is forthcoming.

Estimates of the quantity β for active c-w seekers range[3] from 10^{-14} to 10^{-16}. Possible values of I are 10^{-4} to 10^{-6}. Assuming $\beta = 10^{-15}$, $I = 10^{-4}$, and $\overline{NF}$ = 18 db, one can see that the maximum useful value of $\overline{P}$ is about 25 watts.

There are, of course, tricks that can be tried to reduce noise. Some of these are mentioned in Ref. 3.

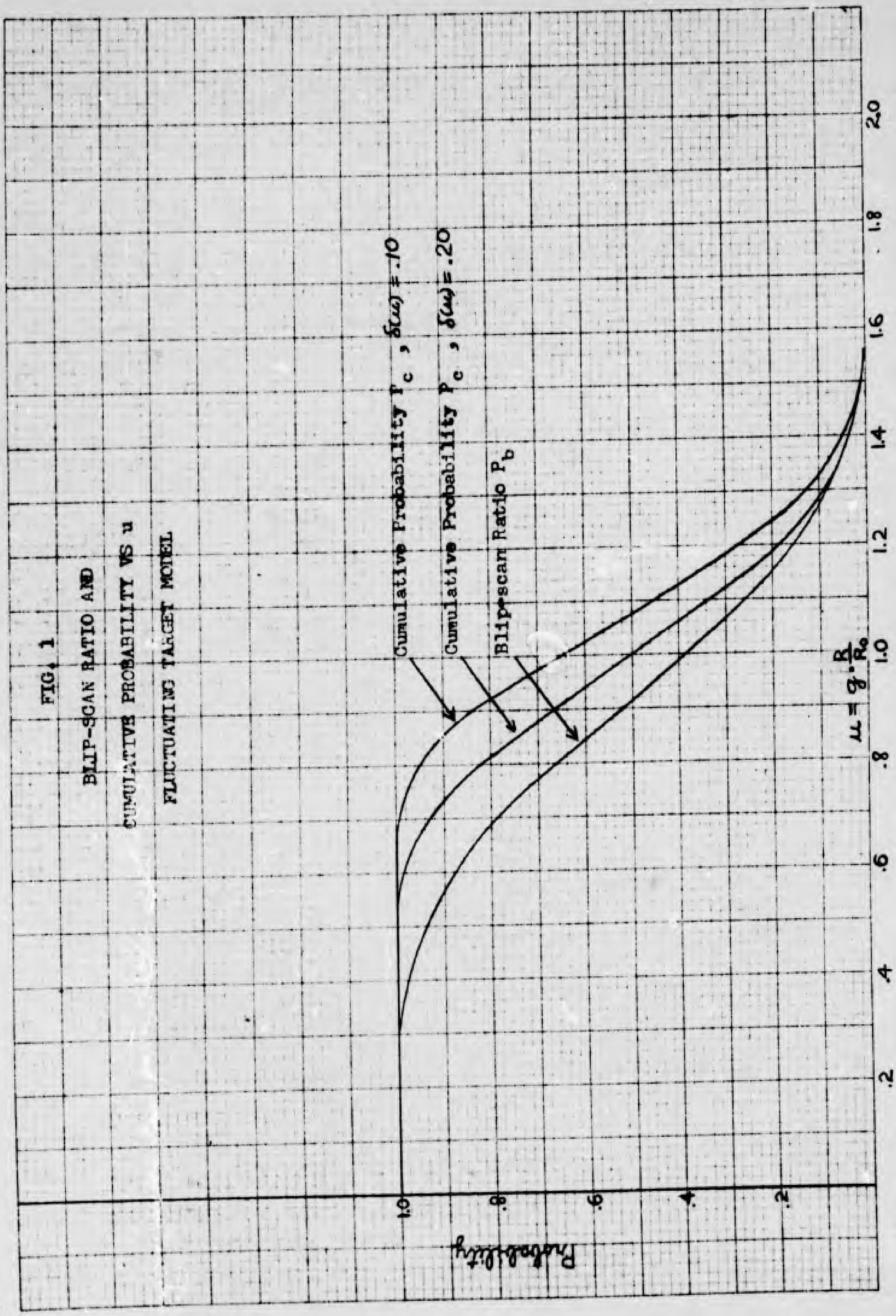

FIG. 1

BLIP-SCAN RATIO AND

CUMULATIVE PROBABILITY VS u

FLUCTUATING TARGET MODEL

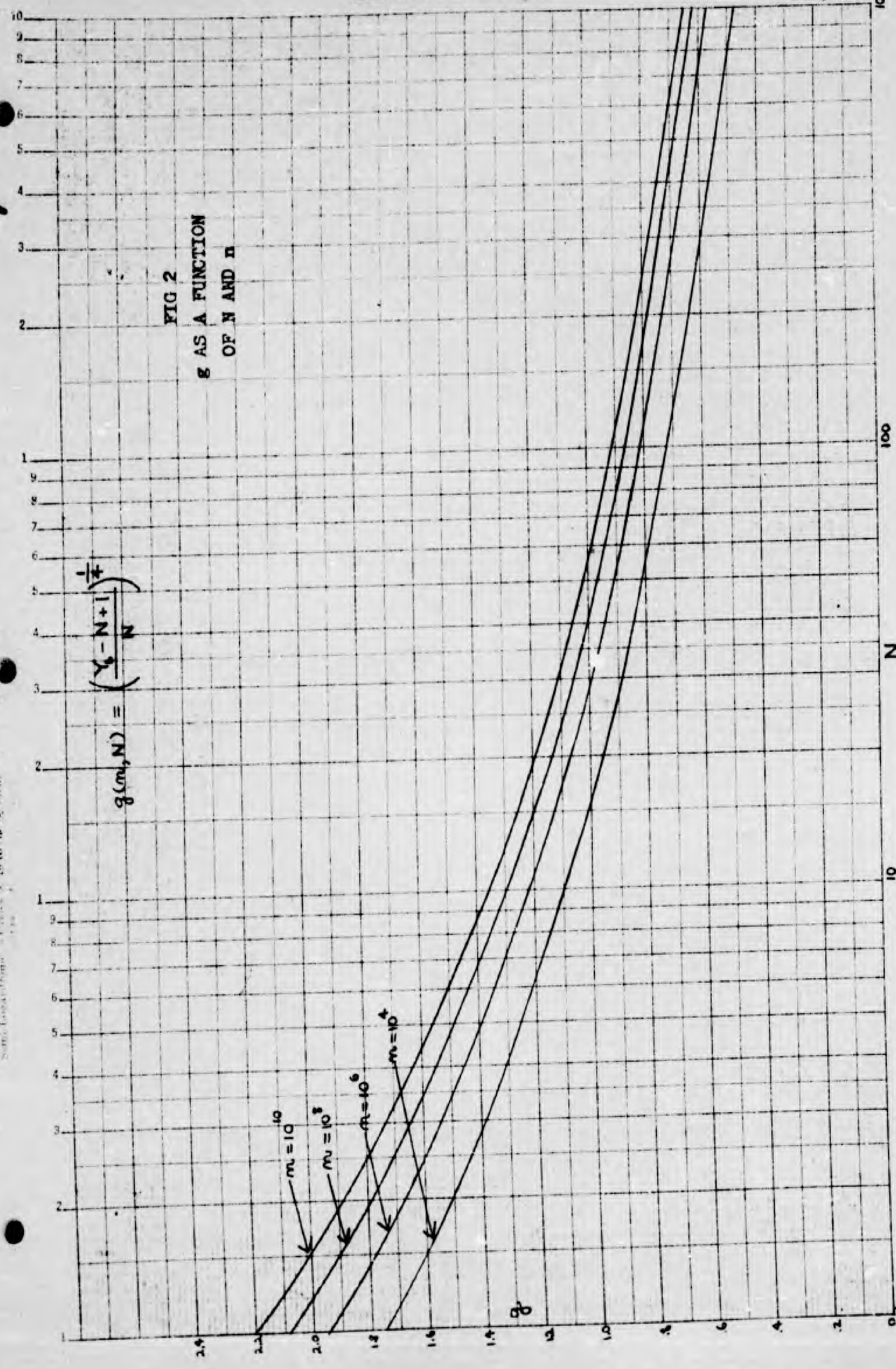

FIG 2
g AS A FUNCTION
OF N AND n

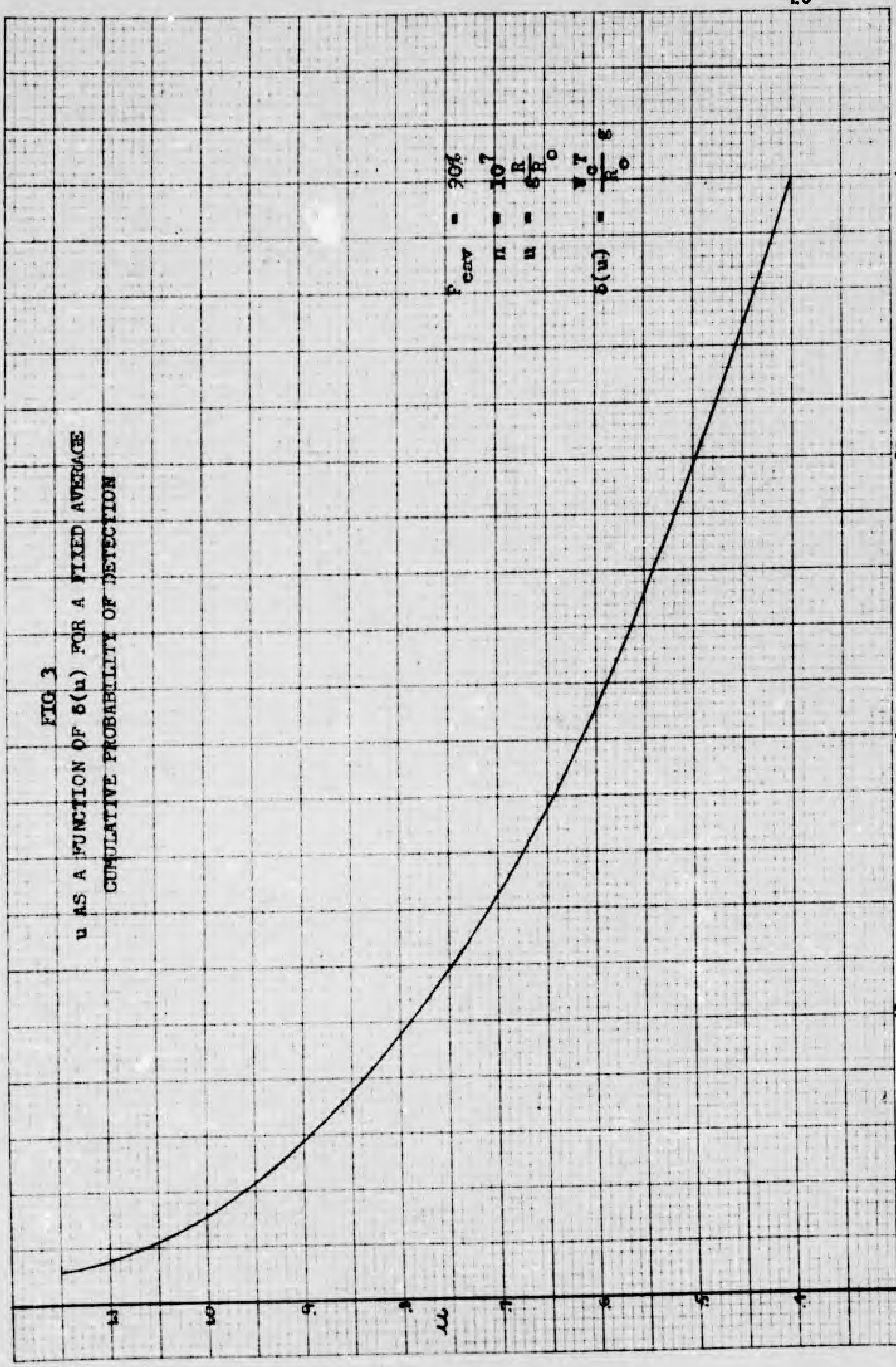

FIG 3

u AS A FUNCTION OF δ(u) FOR A FIXED AVERAGE CUMULATIVE PROBABILITY OF DETECTION

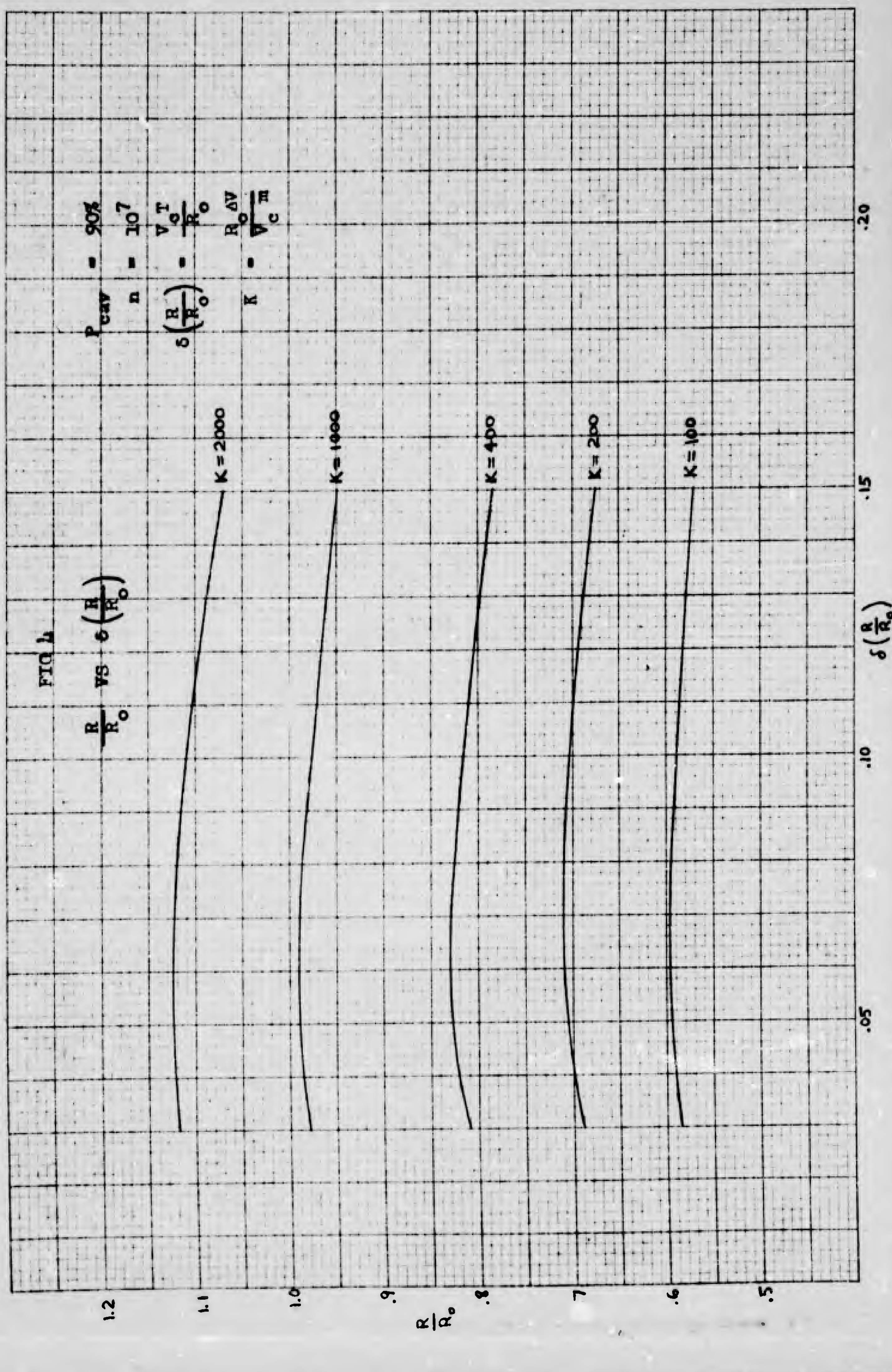
FIG 4
R/R_o VS δ(R/R_o)
P_cav = 90%
n = 10^7
δ(R/R_o) = V_c T / R_o
K = R_o ΔV / V_c m
K = 2000
K = 1000
K = 400
K = 200
K = 100
.05
.10
.15
.20
δ(R/R_o)
1.2
1.1
1.0
.9
.8
.7
.6
.5
R/R_o

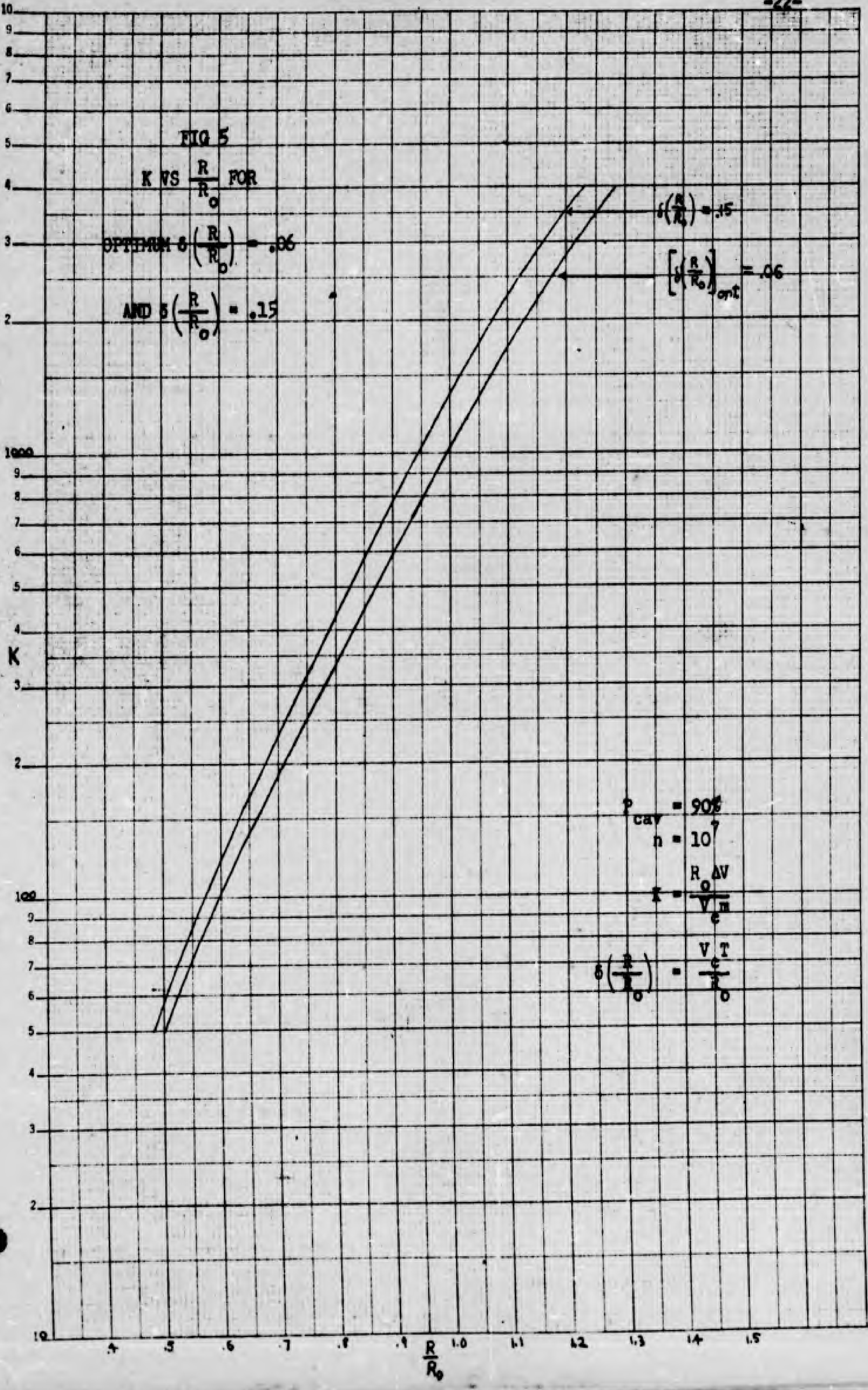
FIG 5
K VS R/R0 FOR
OPTIMUM δ(R/R0) = .06
AND δ(R/R0) = .15
δ(R/R0) = .15
[δ(R/R0)]opt = .06
P cav = 90%
n = 10^7
K = R0 ΔV / Ve n
δ(R/R0) = Ve T / R0
K
R/R0
10
9
8
7
6
5
4
3
2
1000
100
10
.4
.5
.6
.7
.8
.9
1.0
1.1
1.2
1.3
1.4
1.5

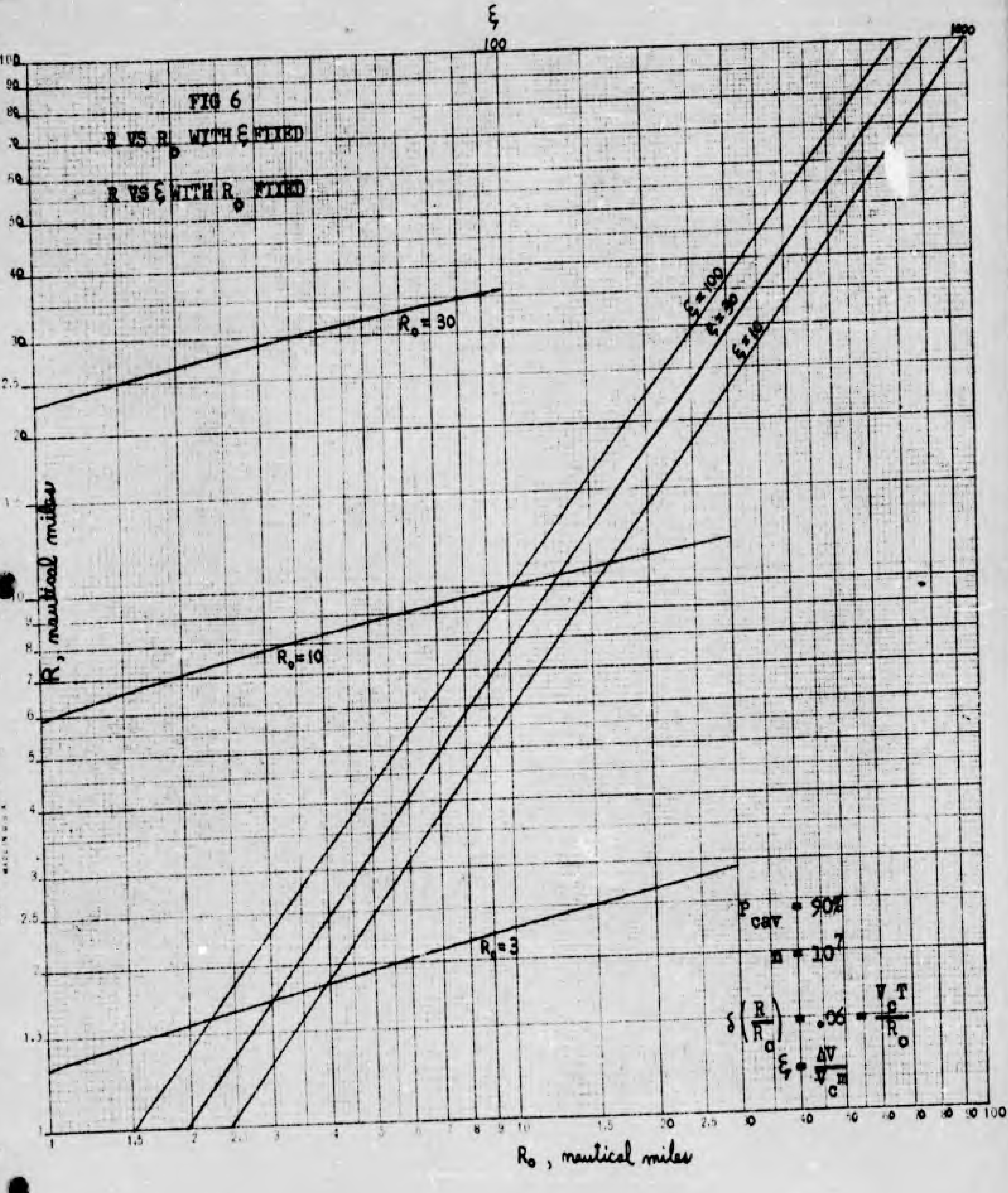
ξ
100
1000
FIG 6
R VS R_o WITH ξ FIXED
R VS ξ WITH R_o FIXED
R_o = 30
R_o = 10
R_o = 3
ξ = 100
ξ = 30
ξ = 10
R, nautical miles
R_o, nautical miles
P_{cav} = 90%
n = 10^7
$\delta\left(\frac{R}{R_o}\right)$ = .06 = $\frac{V_c T}{R_o}$
ξ = $\frac{\Delta V}{V_{cn}}$

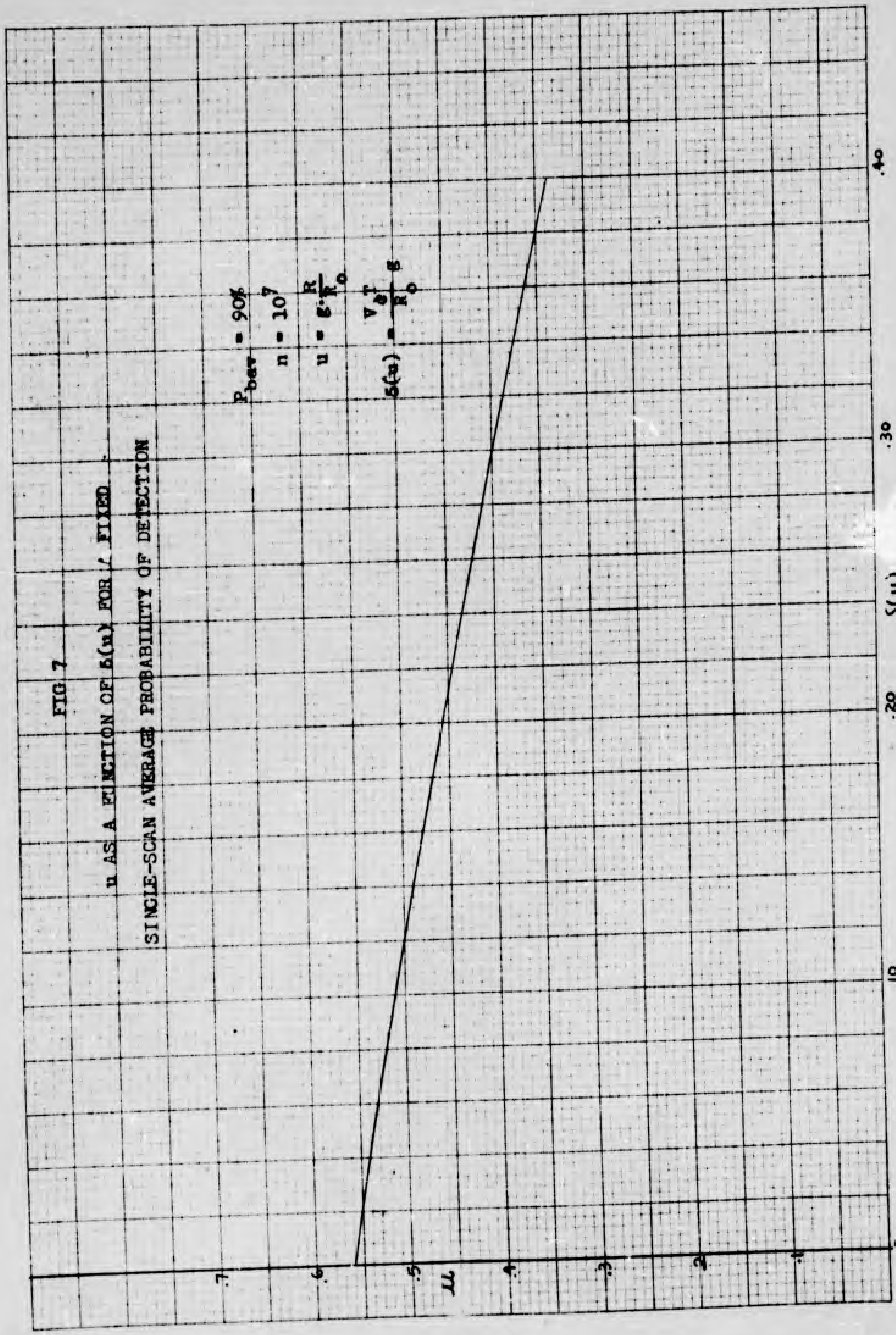
FIG 7
u AS A FUNCTION OF δ(u) FOR P FIXED
SINGLE-SCAN AVERAGE PROBABILITY OF DETECTION
P_{bav} = 90%
n = 10^7
u = $\epsilon \cdot \frac{R}{R_o}$
0
.10
.20
.30
.40
δ(μ)
.1
.2
.3
.4
.5
.6
.7
μ

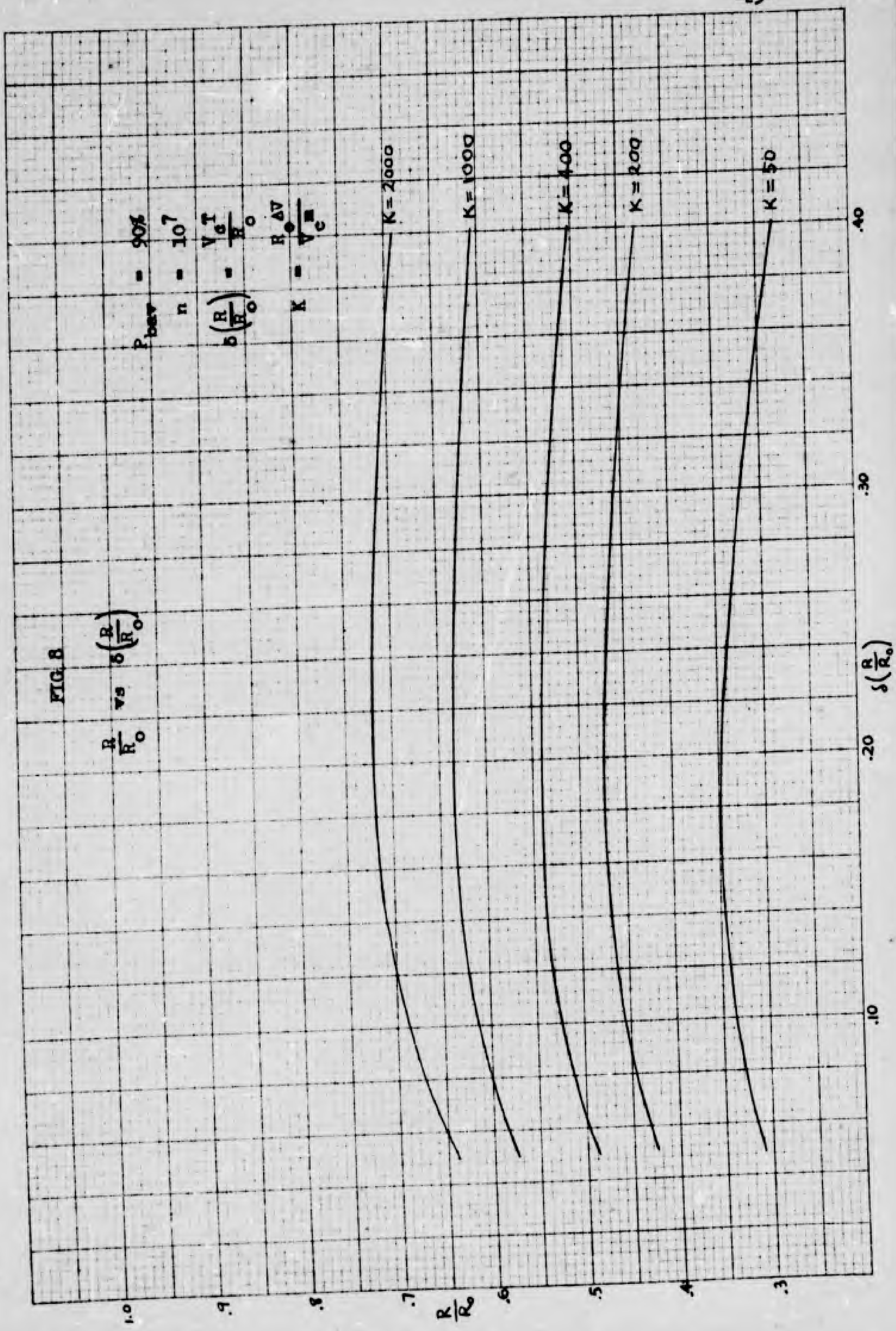
FIG. 8
R/R_o vs δ(R/R_o)
P_bev = 90%
n = 10^7
δ(R/R_o) = V_d T / R_o
K = R_o ΔV / V_c m
K = 2000
K = 1000
K = 400
K = 200
K = 50
.10
.20
.30
.40
δ(R/R_o)
1.0
.9
.8
.7
.6
.5
.4
.3
R/R_o

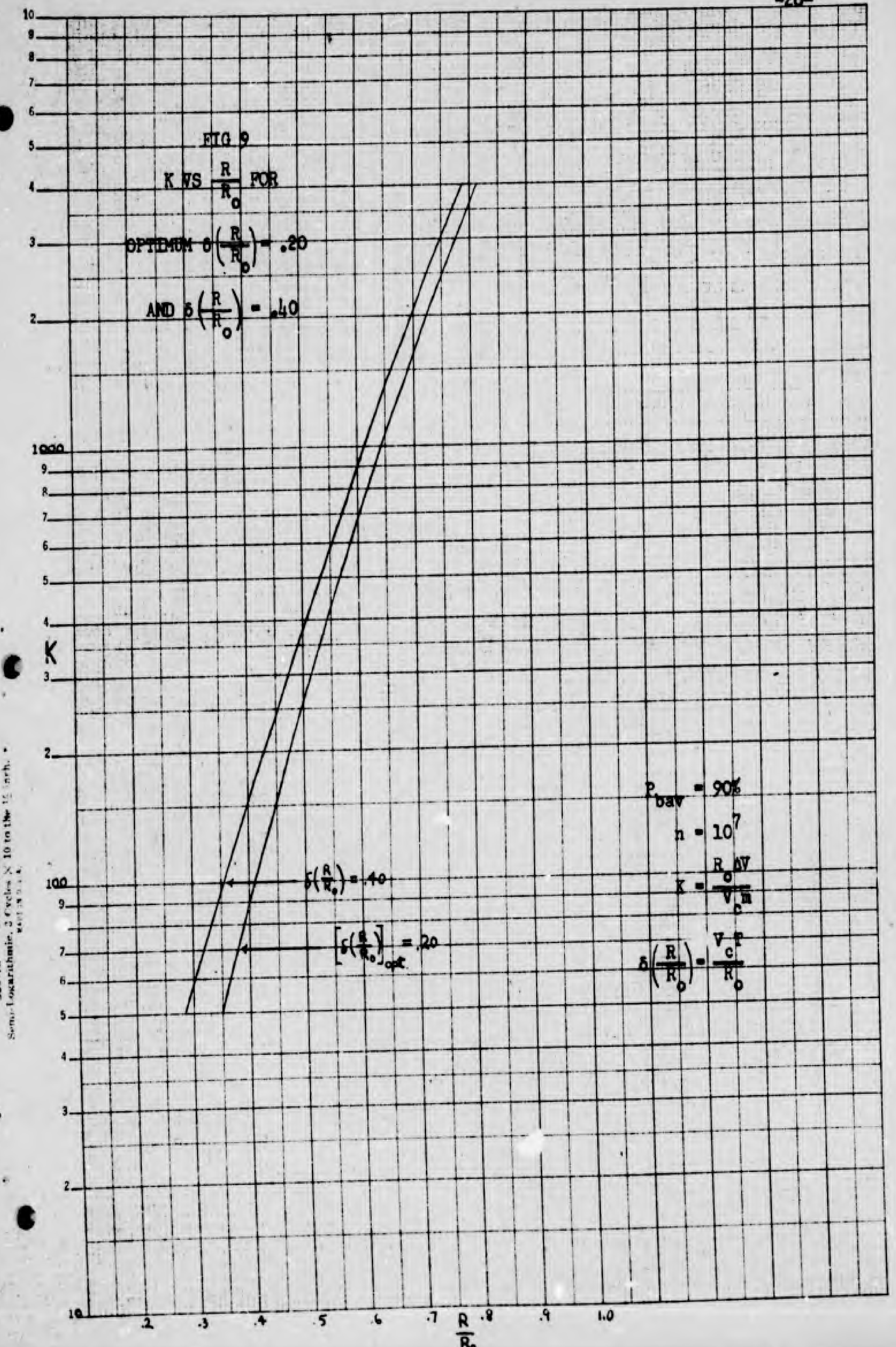
FIG 9
K VS R/R_o FOR
OPTIMUM δ(R/R_o) = .20
AND δ(R/R_o) = .40
K
δ(R/R_o) = .40
[δ(R/R_o)]_opt = .20
P_bav = 90%
n = 10^7
K = R_o ΔV / V_c m
δ(R/R_o) = V_c T / R_o
R/R_o
.2
.3
.4
.5
.6
.7
.8
.9
1.0
KEUFFEL & ESSER CO.
359-73
Semi-Logarithmic, 3 Cycles X 10 to the ½ inch.

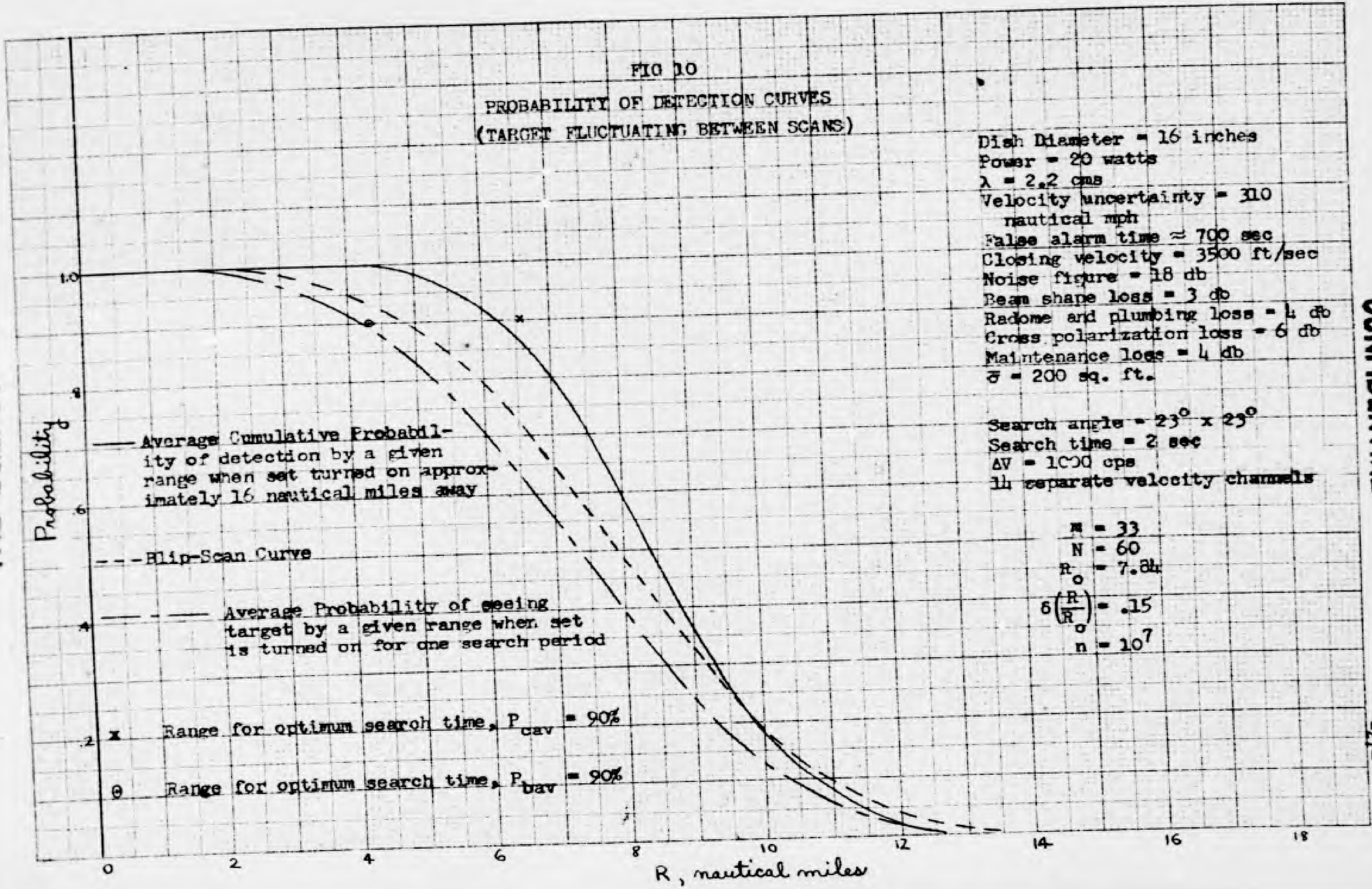
FIG 10
PROBABILITY OF DETECTION CURVES
(TARGET FLUCTUATING BETWEEN SCANS)
Dish Diameter = 16 inches
Power = 20 watts
λ = 2.2 cms
Velocity uncertainty = 310 nautical mph
False alarm time ≈ 700 sec
Closing velocity = 3500 ft/sec
Noise figure = 18 db
Beam shape loss = 3 db
Radome and plumbing loss = 4 db
Cross polarization loss = 6 db
Maintenance loss = 4 db
σ = 200 sq. ft.
Search angle = 23° x 23°
Search time = 2 sec
ΔV = 1000 cps
14 separate velocity channels
m = 33
N = 60
R_o = 7.84
δ(R/R_o) = .15
n = 10^7
— Average Cumulative Probability of detection by a given range when set turned on approximately 16 nautical miles away
- - - Blip-Scan Curve
— - — Average Probability of seeing target by a given range when set is turned on for one search period
x Range for optimum search time, P_cav = 90%
θ Range for optimum search time, P_bav = 90%
Probability
1.0
.8
.6
.4
.2
0
2
4
6
8
10
12
14
16
18
R, nautical miles

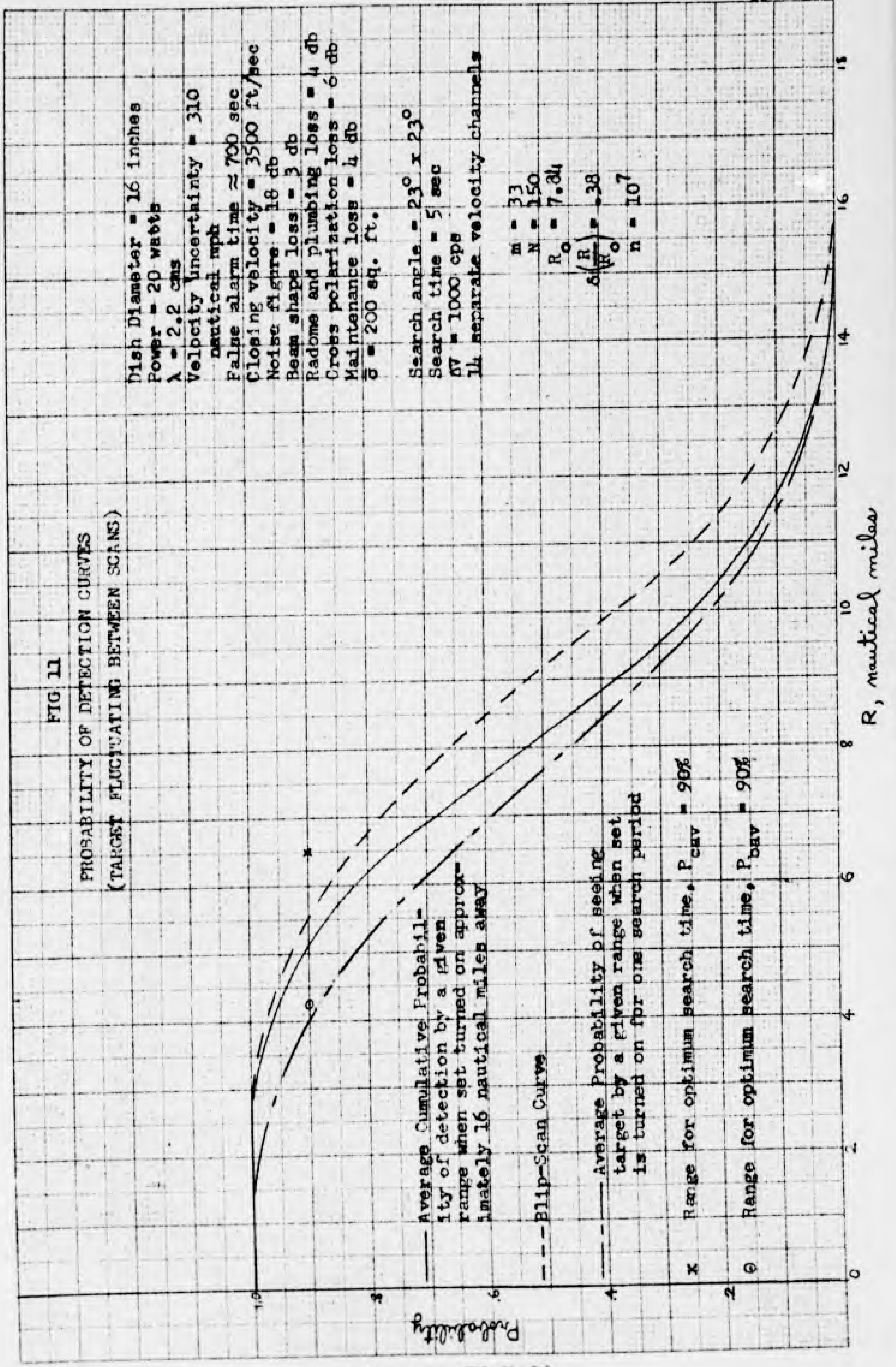
FIG 11
PROBABILITY OF DETECTION CURVES
(TARGET FLUCTUATING BETWEEN SCANS)
Dish Diameter = 16 inches
Power = 20 watts
λ = 2.2 cms
Velocity Uncertainty = 310 nautical mph
False alarm time ≈ 700 sec
Closing velocity = 3500 ft/sec
Noise figure = 18 db
Beam shape loss = 3 db
Radome and plumbing loss = 4 db
Cross polarization loss = 6 db
Maintenance loss = 4 db
σ̄ = 200 sq. ft.
Search angle = 23° x 23°
Search time = 5 sec
Δν = 1000 cps
14 separate velocity channels
m = 33
N = 150
R_o = 7.34
$\delta\left(\frac{R}{R_o}\right)$ = .38
n = 10^7
—— Average Cumulative Probability of detection by a given range when set turned on approximately 16 nautical miles away
- - - Blip-Scan Curve
—·— Average Probability of seeing target by a given range when set is turned on for one search period
x Range for optimum search time, P_{cmv} = 90%
⊙ Range for optimum search time, P_{bsv} = 90%
1.0
.8
.6
.4
.2
Probability
0
2
4
6
8
10
12
14
16
R, nautical miles

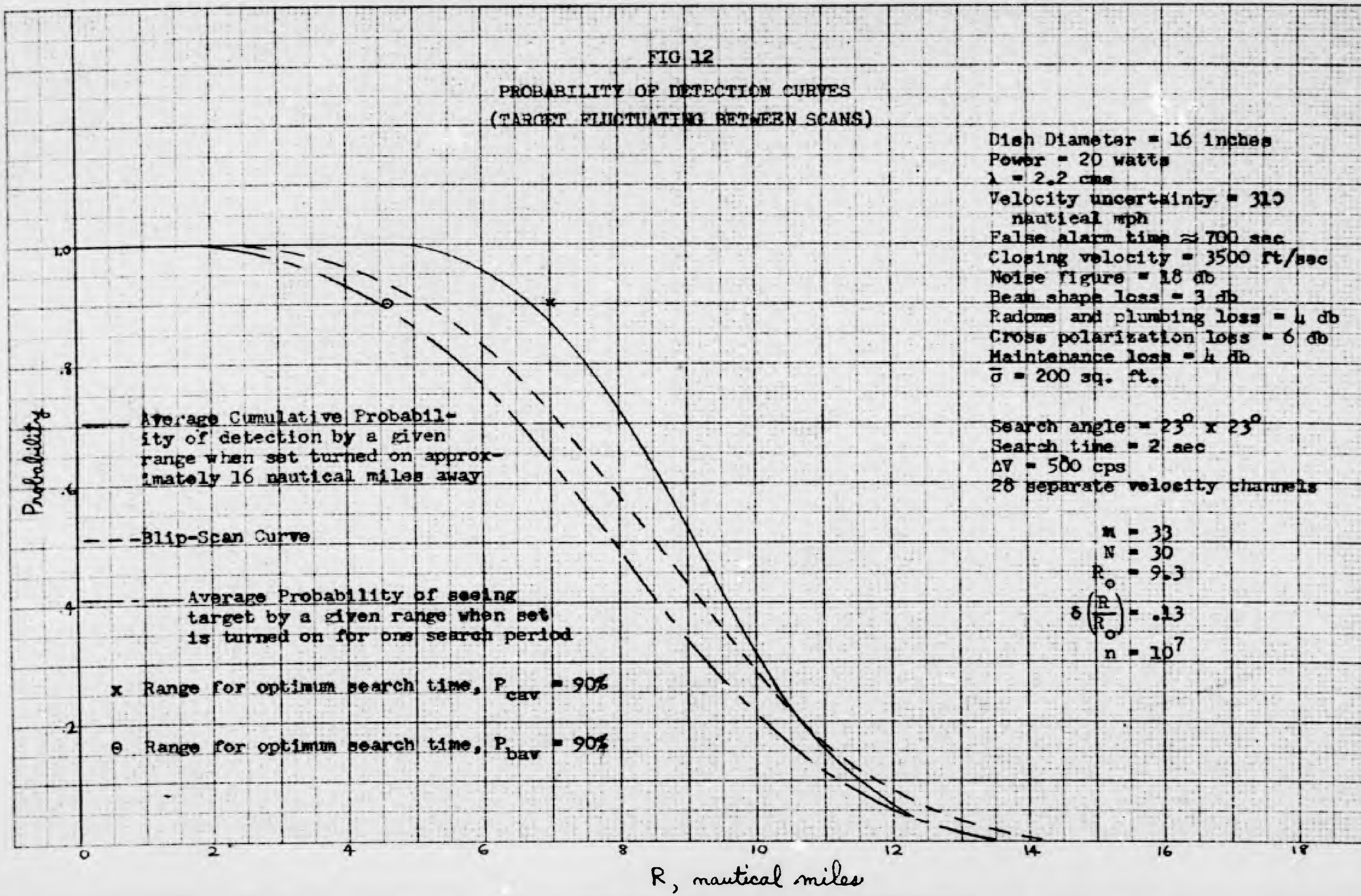

FIG 12

PROBABILITY OF DETECTION CURVES

(TARGET FLUCTUATING BETWEEN SCANS)

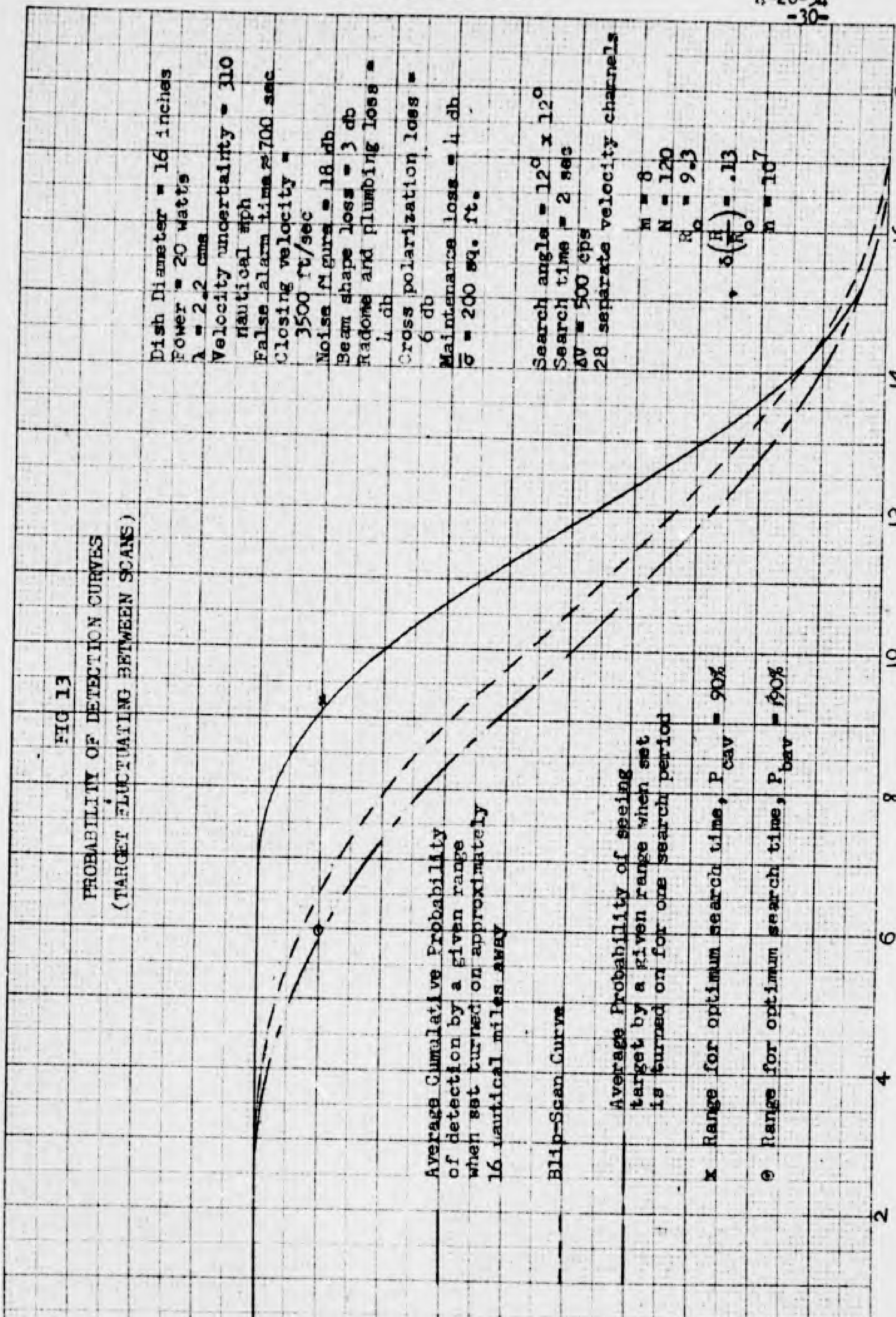
FIG 13
PROBABILITY OF DETECTION CURVES
(TARGET FLUCTUATING BETWEEN SCANS)
Dish Diameter = 16 inches
Power = 20 watts
λ = 2.2 cms
Velocity uncertainty = 310 nautical mph
False alarm time ≈ 700 sec
Closing velocity = 3500 ft/sec
Noise figure = 18 db
Beam shape loss = 3 db
Radome and plumbing loss = 4 db
Cross polarization loss = 6 db
Maintenance loss = 4 db
σ = 200 sq. ft.
Search angle = 12° x 12°
Search time = 2 sec
ΔV = 500 cps
28 separate velocity channels
m = 8
N = 120
R₀ = 9.3
δ(R/R₀) = .13
n = 10⁷
Average Cumulative Probability of detection by a given range when set turned on approximately 16 nautical miles away
Blip-Scan Curve
Average Probability of seeing target by a given range when set is turned on for one search period
x Range for optimum search time, P cav = 90%
⊙ Range for optimum search time, P bav = 90%
Probability
R, nautical miles
0
2
4
6
8
10
12
14
16
18
.2
.4
.6
.8
1.0

FIG 14

PROBABILITY OF DETECTION CURVES

(NON-FLUCTUATING OR VERY RAPIDLY FLUCTUATING TARET MODEL)

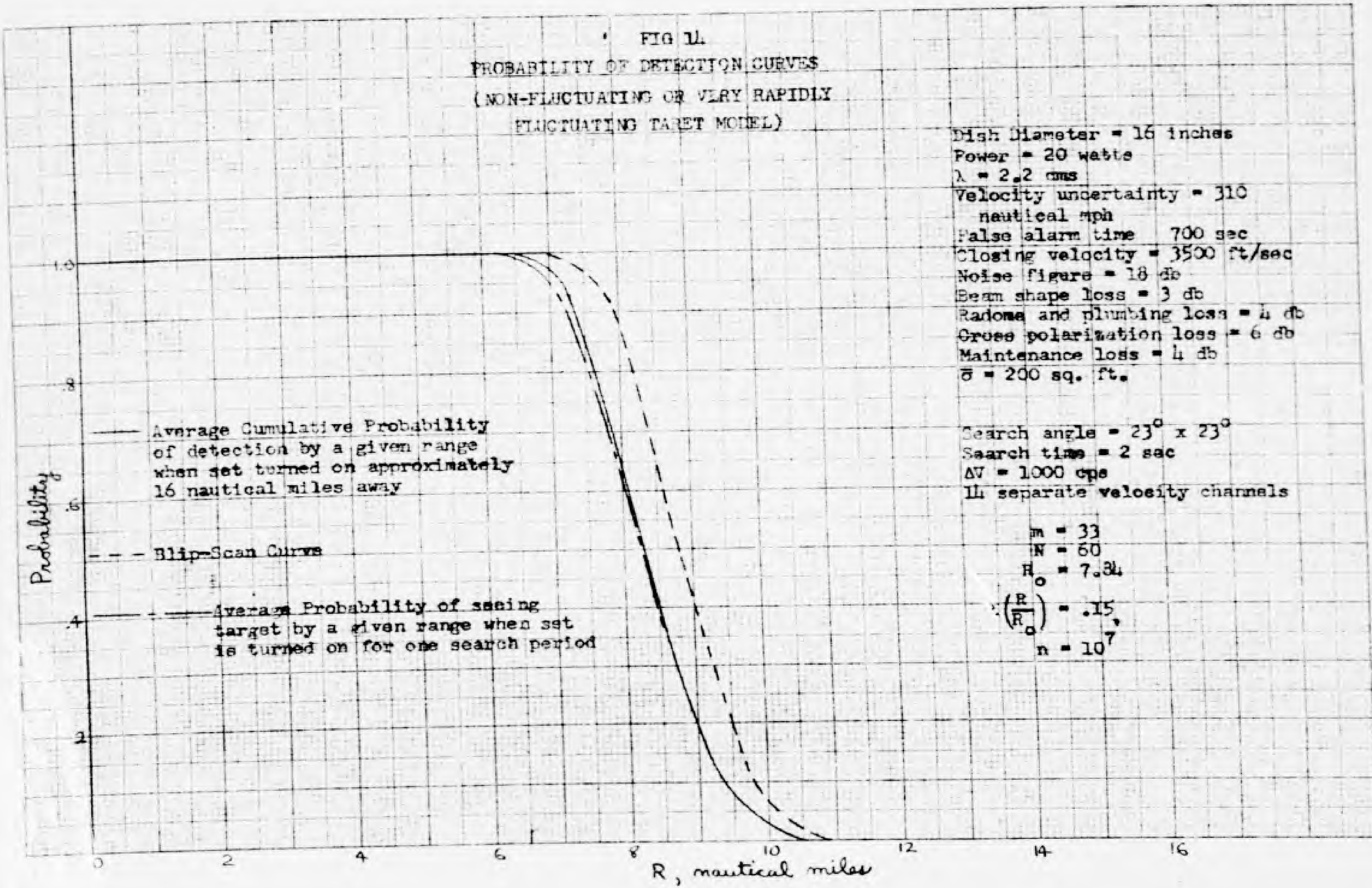

REFERENCES

1. Marcum, J. I., A Statistical Theory of Target Detection by Pulsed Radar, The RAND Corporation, Research Memorandum RM-754, April 25, 1952.

2. Swerling, P., Probability of Detection for Fluctuating Targets, The RAND Corporation, Research Memorandum RM-1217, March 17, 1954.

3. Graham, W. B., J. D. Mallett, and R. C. Emerson, The Capabilities and Limitations of Some MTI Radar Systems, The RAND Corporation, Research Memorandum RM-527, February 1, 1951.